Microporous and Mesoporous Materials 236 (2016) 28–37

Contents lists available at ScienceDirect

Microporous and Mesoporous Materials

journal homepage: www.elsevier.com/locate/micromeso

Effect of carbonization temperature on adsorption property of ZIF-8 derived nanoporous carbon for water treatment

Zahra Abbasi [a], Ezzatollah Shamsaei [a], Soo Kwan Leong [a], Bradley Ladewig [a, b], Xiwang Zhang [a], Huanting Wang [a, *]

[a] Department of Chemical Engineering, Monash University, Clayton, Victoria, 3800, Australia
[b] Department of Chemical Engineering, Imperial College London, Exhibition Road, London, SW7 2AZ, United Kingdom

ARTICLE INFO

Article history:
Received 20 June 2016
Received in revised form
7 August 2016
Accepted 22 August 2016
Available online 23 August 2016

Keywords:
Adsorption
Metal organic framework
ZIF-8
Carbonization
Water treatment

ABSTRACT

The heat treatment effect on the adsorption capabilities of nanoporous carbon particles derived from Zeolitic Imidazolate Framework-8 (ZIF-8) was investigated at 600, 1000 and 1200°C in this study. The results showed that heat treatment at 1000°C had a significant effect on the adsorption capacity of ZIF-8 (almost 10 times) for the removal of methylene blue (MB) dye from water. Nanoporous carbons were synthesized by direct carbonization of ZIF-8. SEM and TEM images showed that the carbon resulting from ZIF-8 carbonization at various temperatures retained the original structure and morphology of ZIF-8. The carbon nanoparticles carbonized at 1000°C exhibited outstanding adsorption capacities (186.3 mg/g) compared to nanoparticles carbonized at 600°C (49.5 mg/g) and 1200°C (36.7 mg/g) as well as ZIF-8 (19.5 mg/g) due to the change in surface charge and pore size distribution. The surface functionalities of materials were also characterized by Raman Spectroscopy, N_2 adsorption-desorption, FTIR and TGA. The surface charge of the carbon particles changed from positive (ZIF-8) to negative as a result of conversion to carbon confirmed by zeta potential of the samples. The ZIF-8 derived carbon nanoparticles were found to be efficient adsorbents for water treatment purposes due to the satisfactory adsorption properties such as high adsorption capacity and good wettability.

1. Introduction

Nanoporous carbon materials have promising characteristics such as high surface area, good chemical and thermal stabilities, fast kinetics as well as tendency to organic contaminants which makes them attractive for adsorption and separation applications [1,2]. For example, they have been used as supercapacitor [3–5], catalyst support [6–8] and adsorbent for hydrogen storage [9] as well as CO_2 capture [2,10–12]. In particular, they are widely used as adsorbents to remove organic and heavy metal contaminants from water in water treatment and purification [13–18].

A wide range of methods have been developed to prepare nanoporous carbons, including chemical vapor deposition (CVD) [19], templating [20,21] and chemical or physical activation method [22]. Inorganic hard templates like zeolites and mesoporous silica [23,24] and Soft template method [25,26] have been utilized to prepare nanoporous carbon particles. In addition, organic spheres are considered as common starting materials for the production of carbon nanoparticles through carbonization [27]. Recently, porous metal organic frameworks (MOFs) with uniform pore sizes, highly crystalline structures, and high surface areas have been studied as adsorbents and for use as precursors of nanoporous carbons [3,4,27–33].

Different kinds of metal organic framework materials have been investigated for the adsorption of dye molecules such as methylene blue from water and wastewater. However, their adsorption capacity is low compared to nanoporous carbons. For example, CU-BTC [BTC = 1,3,5-benzenetricarboxylate] also known as HKUST-1 as well as Fe3O4@MIL-100(Fe) have been studied for the removal of MB from water and they showed adsorption capacities of 15.28 μmol/g (equivalent to 4.8 mg/g) and 49.4 mg/g respectively [34,35]. Among MOF materials, zeolitic immidazolate frameworks (ZIFs) are a class of MOFs that show many outstanding features like high thermal and chemical stability. ZIF-8 is one of mostly studied ZIFs, and has a molecular formula of Zn(2-methylimidazolate)$_2$ and sodalite-related zeolitic structure; it is composed of six membered-

* Corresponding author.
E-mail address: huanting.wang@monash.edu (H. Wang).

http://dx.doi.org/10.1016/j.micromeso.2016.08.022
1387-1811/

ring pore windows (0.34 nm) and larger pores (1.14 nm) and has been reported as an adsorbent for the removal of various pollutants from water [31]. It is worth noting that ZIF-8 has fast adsorption rate and high adsorption capacity for the removal of benzotriazols from aqueous solutions [36]; however, this material has very low adsorption capacity for the removal of methylene blue dye from water. The low MB uptake could be due to the net positive charge of ZIF-8 and its small pores which hinder adsorption of large and positively charged molecules such as methylene blue. Therefore, much work has been carried out to convert MOFs (ZIFs) into nanoporous carbons to achieve desirable adsorption properties [27]. MOFs have large carbon contents and play the roles of sacrificial template and carbon precursor during carbonization process [4].

To date, there have been a few reports in the literature about the utilization of MOF derived nanoporous carbon for water treatment. For instance, nanoporous carbons derived from ZIF-67, MIL-100 and MOF-5 were prepared, and they had improved adsorption capacity for the removal of MB from water [1,37,38]. The nanoporous carbon was also obtained by carbonizing ZIF-8 at 800°C [2,39]. However, the methylene blue adsorption capacity of ZIF-8-derived carbon was low (59 mg/g), which was because the carbonization temperature (800°C) was lower than the boiling point of Zn (908°C), limiting the surface area and pore volume of the nanoporous carbon [40,41].

Even after steam treatment was conducted at 800°C to promote the porous carbon network, the adsorption capacity of the resulting carbon was still low (105.7 mg/g). This indicates the importance of carbonization temperature on the adsorption property of ZIF-8-derived nanoporous carbon.

In this study, we focused on the effect of carbonization temperature on the adsorption capacity of ZIF-8 for water treatment, particularly the removal of methylene blue as a model dye pollutant from water. The changes of the ZIF-8 characteristics due to carbonization such as morphology, surface area and pore size distribution, surface charge, and surface functional groups were studied. Our studies showed that the ZIF-8 derived nanoporous carbon prepared at 1000°C had significantly greater adsorption capacity than that at lower temperature.

2. Materials and methods

2.1. Materials

Zinc nitrate hexahydrate ($Zn(NO_3)_2.6H_2O$), 2-methylimidazole (Hmim) (99%), brilliant green (BG), rhodamine B (RhB) and methyl orange (MO) were purchased from Sigma Aldrich. Methylene blue was purchased from Merck. All chemicals were used as received without any purification. ZIF-8 parent was synthesized by environmentally friendly synthesis method in aqueous solution reported by Koji Kida et al. [42]. Typically, 0.744 g (2.5 mmol) of $Zn(NO_3).6H_2O$ and 12.3 g (0.15 mol) of Hmim were dissolved in 10 ml and 90 ml of deionized water respectively. After being stirred for 24 h, ZIF-8 nanocrystals were collected by washing with deionized water and centrifuging (8000 rpm, 30 min) for three times and then dried at 80°C overnight. ZIF-8 was directly carbonized at various temperatures (600, 1000 and 1200°C) under a flow of argon gas. The temperatures rose steadily from room temperature to the target temperatures with a heating rate of 5°C/min. After reaching the target temperatures, the powders were annealed at the target temperatures for 6 h. These products were denoted as CZIFs (carbonized ZIF-8) and as CZIF600, CZIF1000 and CZIF1200 to indicate the heat treatment temperatures.

After the carbonization the nanoporous carbon samples were directly used for characterization and adsorption experiments without any further activation or acid washing to present a simple and environmentally friendly approach.

2.2. Characterization

Nitrogen adsorption and desorption isotherms were measured at liquid nitrogen temperature (77 K) using an accelerated surface area and porosimetry system (ASAP 2010, Micromeritics, USA) for surface area measurements. The crystal structures of the samples were identified using an X-ray diffractometer (Miniflex 600, Rigaku) with Cu Kα radiation at 40 kV and 20 mA over the 2θ range of 2–90°. The morphology of the adsorbent materials was observed using a scanning electron microscope (FEI Nova NanoSEM 450 FEG SEM). Transmission electron microscopy of the carbonized ZIFs was done by FEI Tecnai G2 T20 TWIN TEM under the working conditions of 200 kV. Thermogravimetric analyses (TGA) were carried out on a SETARAM (TGA 92) device from 30 to 1200°C at a heating rate of 10°C/min and under Ar flow. The zeta potentials of the samples were determined using a Zetasizer Nano (Malvern) at a pH range of 1–11. The powders were dispersed by sonication in water with a concentration of 0.5mg/10 ml and the dispersion was used for zeta potential measurements. Since ZIF-8 is not stable in acidic conditions, the pH adjustment for ZIF-8 was done only for basic conditions to measure zeta potentials.

The Raman spectra were recorded on WITEC Alpha 300 confocal micro-Raman system equipped with a 532 nm laser source and 100X objective lens. The concentration of methylene blue (MB), brilliant green (BG), rhodamine b (RhB) and methyl orange (MO) were measured using a UV_vis spectrophotometer (UVmini-1240, Shimadzu) at wavelengths of 665, 625, 554 and 464 nm, respectively, which correspond to the maximum adsorption of the dyes.

FTIR spectra of the samples were recorded using an attenuated total reflectance (ATR) Fourier Transform Infrared (FTIR) (Perkin Elmer, USA) in the range of 500–4000 cm^{-1} at an average of 32 scans with a resolution of 4 cm^{-1}.

2.3. Adsorption experiments

Adsorption on the prepared samples was carried out in batch experiments. The adsorption capacity of these materials was evaluated by adsorption of an organic cationic dye methylene blue (MB) in aqueous solution. Rhodamine B (RhB), brilliant green (BG) and methyl orange (MO) were also used to examine the carbonized samples for adsorption of different types of dye molecules. However, the adsorption isotherms and kinetics were conducted for methylene blue only as a model dye compound. An aqueous stock solution of MB ($C_{16}H_{18}N_3SCl$, MW: 373.9), RhB, BG and MO with 1000 ppm concentration was prepared in milli-Q water. Aqueous solutions with different concentrations of dyes were prepared by successive dilution of the stock solution with water. For isotherm experiments specific amount of adsorbents (10 mg) was put in the aqueous dye solutions (20 ml) having fixed concentrations from 100 ppm to 500 ppm. The solutions containing the adsorbents were mixed for 24 h at room temperature (22°C).

For kinetic experiments 10 mg of adsorbent was put in 20 ml dye solution with 100 ppm concentration of MB. Then the dye solutions containing the adsorbents were mixed well with magnetic stirring and maintained for a fixed time (5 min–24 h) at room temperature (22°C).

After adsorption for a pre-determined time, the solutions were separated from the adsorbents with a syringe filter (Nylon, hydrophobic, 0.45 μm). The adsorption experiments were done without any pH adjustment and at the natural pH of the solution i.e. 5.5. The dye solution was prepared to the desired concentrations using Milli-Q water.

3. Results and discussions

3.1. Characterization of nanoporous carbon particles

To examine the crystal phase transformation of ZIF-8 under the treatment conditions, X-ray diffraction (XRD) analysis was conducted. Fig. 1 shows the XRD pattern of as synthesized ZIF-8 and carbonized materials. As the temperature increases ZnO is produced during the carbonization and then reduces to Zn by carbon. Thereafter, at temperatures above the boiling point of Zn (908°C), Zn evaporates and leaves with the Ar flow [40,41]. Therefore, at 1000°C, no diffraction peaks of Zn impurities can be seen [32] and the two broad peaks at $2\theta = 23^\circ$ and 44° represent the characteristics of amorphous carbon [3,41]. The reduced Zn probably plays the role of a template for the formation of nanoporous carbon. During the carbonization, reduction of ZnO by carbon leads to the formation of Zn and carbon oxides. The release of these species along with the vaporization of Zn at above 908°C are probably in charge of the formation of the porous framework [43].

In addition, the samples before and after the carbonization were analysed by scanning electron microscopy (SEM) and transmission electron microscopy (TEM) to identify the change in the morphology of the samples. Fig. 2 shows the SEM and TEM of the original and carbonized ZIF-8 (at different temperatures); no change in the morphology and structure of the synthesized ZIF-8 was observed, even after carbonization at high temperatures. This observation is in accordance with literature [1,27].

An adsorbent material must have high internal volume accessible to the components being removed from the solvent. Surface area, in particular the internal surface area, pore size and the nature of the pores strongly affect the adsorption process [44]. The nanoporous structures of prepared carbons were investigated by N_2 adsorption-desorption isotherms (Fig. 3). ZIF-8 and carbonized samples exhibited Type I isotherms with a sharp nitrogen adsorption at low pressures ($P/P_0 < 0.05$) and a small uptake at high pressure ($P/P_0 > 0.9$), indicating a microporous framework with some macropores formed between particles (inter particle voids) [4]. The microporous structure may derive from ZIF-8 as well as

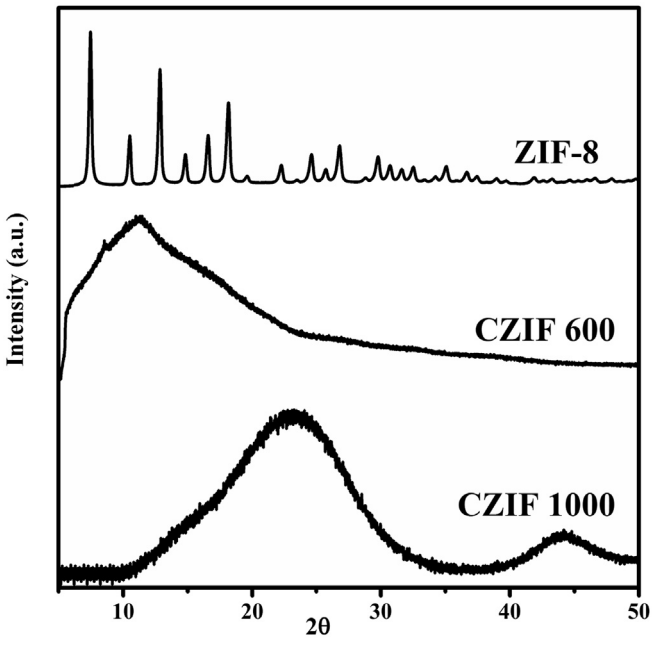

Fig. 1. XRD patterns of synthesized ZIF-8 and its derived carbons at 600°C and 1000°C.

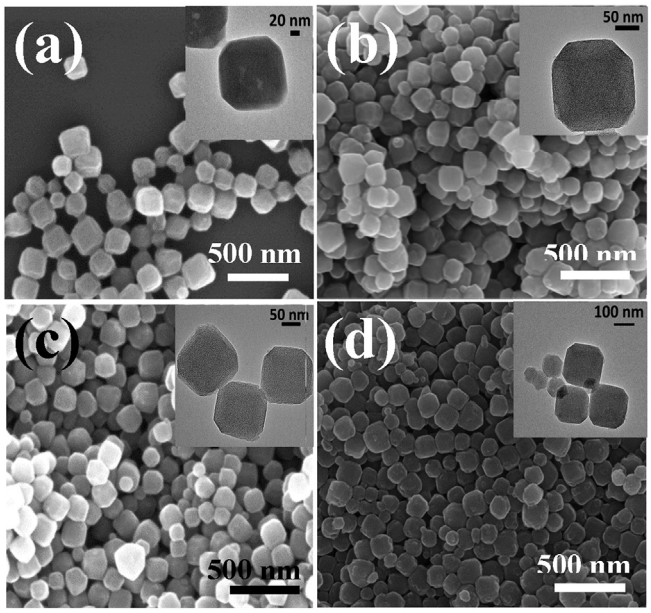

Fig. 2. SEM and TEM images of (a) ZIF-8 (b) CZIF600 (c) CZIF1000 and (d) CZIF1200.

evaporation of Zn during heat treatment [45]. The Brunauer, Emmet and Teller (BET) surface areas and pore volumes are presented in Table 1. It is worth mentioning that after direct carbonization the nano porous carbons still had high surface areas which enhanced their adsorption performances.

As reflected in the table, the surface areas of the carbonized sample at 600°C decreased after carbonization while the surface area of the sample treated at 1000°C increased. Interestingly, ZIF-8 carbonized at 1200°C exhibits a surface area lower than CZIF 1000. This could be due to the densification of porous carbon structure at high temperature, consequently leading to a reduction of the surface area.

For the carbonized samples, the pore size distribution became to some extent broader as a result of carbonization (as evidenced from Fig. 3). Therefore, heat treatment of ZIF-8 resulted in the modification of the pore size distribution and this feature along with the high surface area facilitates the diffusion of MB molecules into the carbon network and helps the increase in adsorption capacity of the materials. The molecular dimension of MB is 1.43 nm × 0.61 nm × 0.4 nm [1] and is within the broad pore size range of the carbonized ZIF-8 shown in Fig. 3. The tails of the isotherm curves for carbonized samples show N_2 uptake at high relative pressures, which could be attributed to condensation effects in externally formed pores between the nanoparticles [11].

The effect of heat treatment on the surface area of ZIF-8 is in consistent with the results reported by Gadipelli et al. [46]. In their study, it was shown that carbonization of MOF-5 (a metal organic framework containing Zn) at temperatures below 900°C, resulted in a decrease in surface area. On the contrary, heat treatment at temperatures higher than the evaporation temperature of Zn (908°C) caused an increase in the surface area. The reason was attributed to the reduction of ZnO with carbon and the evolution of Zn, CO and CO_2 which results in a more porous network. The increase in the surface area and porosity of the carbon materials could be explained with reference to the thermogravimetric analysis of ZIF-8 material as illustrated in Fig. 4.

As shown in Fig. 4, ZIF-8 organic linkers start to decompose at around 500–600°C and the generated Zn species probably block the pores and this results in a lower surface area [45]. However, by

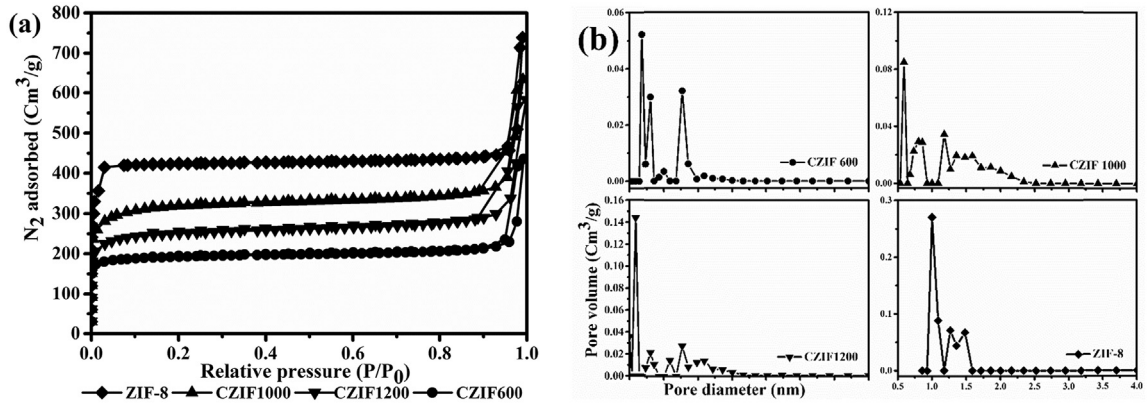

Fig. 3. Nitrogen adsorption-desorption isotherm of ZIF-8 and the nanoporous carbons at 600, 1000 and 1200°C (a) and the corresponding pore size distributions (b). All horizontal axes of pore size distributions have the same scale of ZIF-8 graph i.e. pore diameter is in the range of 0.5–4 nm.

Table 1
Surface area analysis parameters of ZIF-8 and its derived carbons at 600, 1000 and 1200°C.

Sample	BET surface area (m^2/g)	Langmuir surface area (m^2/g)	Total pore volume[a] (Cm^3/g)	Micropore volume (Cm^3/g)
ZIF-8	1384.2	1849	1.1	0.63
CZIF600	625.5	811.9	0.67	0.26
CZIF1000	1043.1	1305	0.98	0.4
CZIF1200	818.7	1037.8	0.9	0.32

[a] At $P/P_0 = 0.99$.

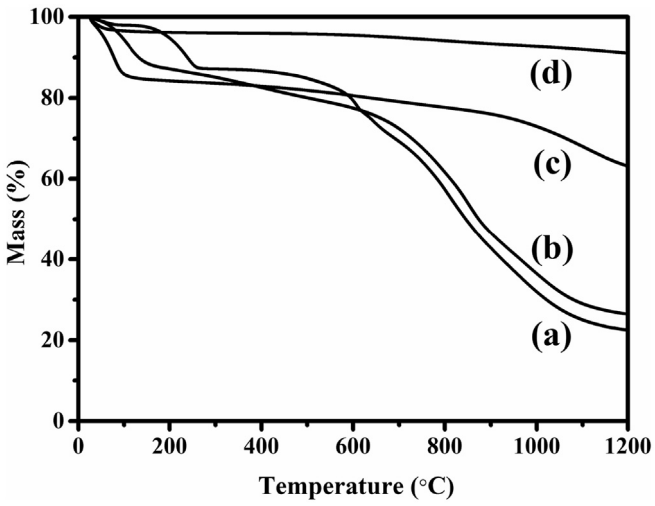

Fig. 4. TGA analysis of ZIF-8 (a), CZIF 600 (b), CZIF 1000 (c) and CZIF1200 (d).

increasing the temperature up to 1000°C, Zn species evaporate at 908°C and this might lead to the production of porosity within the framework which further expands the surface area. The sample carbonized at higher temperature had higher surface area and this shows that the carbonization temperature is very important for the structural formation of the resulting carbon materials. Despite the decrease in the surface area of ZIF-8 after carbonization at 600°C, the surface area of the carbonized sample increased initially with increasing the carbonization temperature (e.g. to 1000°C), but decreased at the carbonization temperature of 1200°C. Similar results have been reported in literature [4]. The pore size of the samples has been defined by density functional theory (DFT) method. As can be seen from Fig. 3, the pore size distribution of the samples changed after carbonization and the distribution covered a broader range of pore sizes with a slight shift towards larger pore diameters. This observation is also similar to the reported study for ZIF-8 carbonization [4]. However, the carbonized ZIF-8 at 1200°C exhibited smaller pore sizes.

The adsorption ability of the surface is determined by an important factor which is called the point of zero charge (pzc) (see Supplementary Material). To determine the point of zero charge of a sample, the zeta potential (measured at various pH values) is plotted against pH. The pH at which the zeta potential is zero is called point of zero charge (pzc). As can be seen from Fig. 5, the pzc of ZIF-8 is above 10. This means the adsorption of positively charged MB molecules on ZIF-8 is only possible at pH levels higher than 10, ignoring the very small accessible pore size of ZIF-8 which

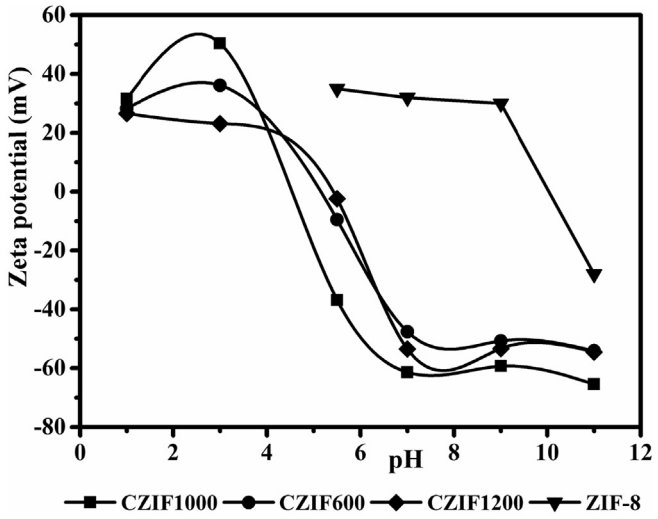

Fig. 5. Zeta potential comparison of ZIF-8 and ZIF derived nano porous carbons over the range pH = 1–11.

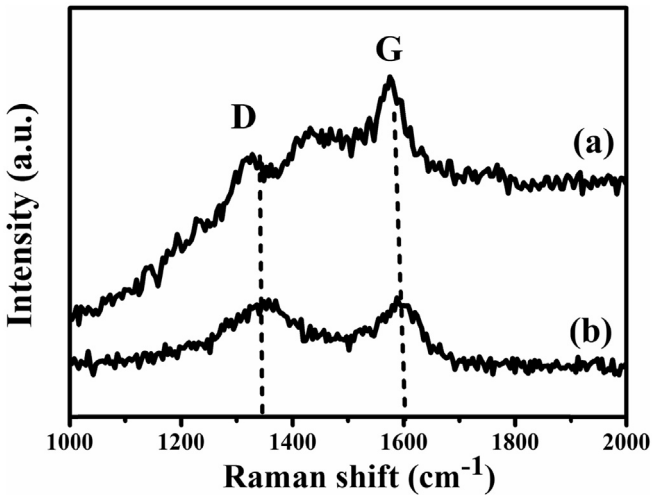

Fig. 6. Raman spectra of (a) CZIF-600 and (b) CZIF-1000.

is too small (0.34 nm) for taking up large MB molecules (1.43 nm × 0.61 nm × 0.4 nm) [47]. In comparison, the points of zero charge for the carbonized ZIF-8 samples are around 4.5–5.5 and as can be seen from figure at pH levels of around 7–8 (the typical pH of industrial wastewaters) the zeta potentials are highly negative which is an indication of potential adsorption capabilities of the synthesized carbon materials for positively charged molecules like methylene blue. It is also observed that the zeta potential of CZIF 1200 is more positive compared with CZIF 600 at pH 5.5, which is the pH at which MB adsorption was conducted. This observation helps to understand the reason behind the low adsorption capacity of CZIF 1200 compared with CZIF 600 and CZIF 1000 despite higher carbonization temperature.

The samples were further analysed by Fourier transform infrared spectroscopy (FTIR) to obtain more information about the local structures and surface functional groups in the carbonized ZIF-8 materials. As shown in Fig. S1 all of the carbon materials show O–H stretching vibrations in the range of 3600–3200 cm^{-1} indicating the presence of hydroxyl groups and adsorbed water molecules [41,48]. The peaks at 1710 and 1620 cm^{-1} are associated with C=O bonds of carboxyl groups and some nitrogen containing species like C=N stretching vibrations in the region 1480-1610 cm^{-1}. The more complicated bands within 1000–1300 cm^{-1} may be addressed to C–O groups [49]. For ZIF-8 material, the peaks observed at 3135 and 2929 are characteristics of aromatic and aliphatic C–H stretch of imidazole and the peaks at 1584, 800–1500 and 421 cm^{-1} are indications of C=N stretch mode, entire imidazole ring vibrations and Zn–N stretch mode respectively [48].

The thermal behaviour of the samples are also shown in the TGA graphs (Fig. 4). At the temperature below 150°C, the mass loss is due to evaporation of adsorbed water molecules in the pores of the materials. Between 400 and 600°C, the mass loss could be due to the framework decomposition which results in carbon consist of gas products such as CO2, CO, as well as formation of metal oxide (ZnO). The mass loss from 900°C onwards, could be attributed to the evolution of CO_2 and CO with Zn through the reduction of ZnO by carbon [46]. This mass loss is more pronounce for ZIF-8 and CZIF 600. In contrast, CZIF 1000 and CZIF 1200 show little mass loss since they already had been treated at 1000 and 1200°C.

The local structures of the resulting nano porous carbons were investigated using Raman spectroscopy and the results are shown in Fig. 6. The carbonization is also confirmed by the Raman spectra considering the graphitic G and D bands at 1350 and 1600 cm^{-1}, respectively [11]. These broadened peaks at 1350 and 1600 cm^{-1} show a disordered carbon network as evidenced by XRD. Typically, the D band illustrates the presence of disordered carbon structures, while the G band is basically attributed to hexagonal graphitic networks in the porous carbon matrix. The intensity ratio of D peak to G peak (I_D/I_G) is an indication of the amount of defects in the carbon materials [11,50]. This value also shows as the carbonization temperature increases, more defects are produced in the carbon matrix. These defects produce more accessible surface areas which promote charge accumulation being advantageous for charge transferring in the adsorption process [50]. Therefore, this feature reflects a favorable characteristic for adsorption capacity of the samples carbonized at higher carbonization temperatures.

3.2. Adsorption study for the removal of methylene blue (MB) dye

The resulting nanoporous carbons were evaluated for their adsorption capabilities with several dyes including MB, RhB, BG and MO to determine the adsorption capability of carbonized ZIF-8 for adsorption of a variety of dyes. For the evaluation of adsorption capacity of the samples, the aqueous solutions of MB, RhB and BG (as positively charged model pollutants) and MO (as negatively charged model pollutant) dyes were used. The dimensions of MB molecule are 1.43 nm × 0.61 nm × 0.4 nm as mentioned previously [1]. Rhodamine B has a molecular dimension of 1.44 nm × 1.09 nm×0.64 nm [51] and methyl orange molecular size is 1.31 nm × 0.55 nm×0.18 nm [52]. The porous carbon prepared by carbonization of ZIF-8 at 1000°C showed adsorption capacities of 84.3, 153.5, 200 and 186.3 mg/g for RhB, MO, BG and MB dyes, respectively. These results show that carbonized ZIF-8 at 1000 C has a tendency to adsorb positively charged dyes, i.e. MB, RhB and BG. However, it has much higher BG and MB adsorption capacity, probably due to the smaller molecular sizes of MB and BG than RhB molecule (1.44 nm × 1.09 nm×0.64 nm) [51]. It is very interesting that CZIF 1000 has also high adsorption capacity for MO which is a negatively charged dye molecule. This feature could be explained by the fact that the molecular size of MO (1.31 nm × 0.55 nm×0.18 nm) [52] is smaller than MB dye (1.43 nm × 0.61 nm × 0.4 nm) [1]. This feature compensates for the negative charge of MO molecule and facilitates MO adsorption on the carbonized ZIF-8 samples.

The adsorption capacities of nanoporous carbons and ZIF-8 for MB adsorption are shown and compared in Fig. 7. Since CZIF1200 had an adsorption capacity lower than CZIF600 and CZIF1000, the adsorption kinetics and isotherms were derived only for the samples carbonized at 600 and 1000°C. The low adsorption capacity of CZIF1200 towards MB dye could be attributed to the more positive surface charge at pH 5.5, as reflected as zeta potential (Fig. 5) and lower surface area as well as smaller pore size distribution after high temperature carbonization (Fig. 3). It is evidenced from Fig. 3 that CZIF1000 has smaller pore sizes and distribution than CZIF600.

It can be seen that the carbonized ZIF-8 materials have significantly higher adsorption capacities in comparison with ZIF-8. It is also observed that the heat treatment temperature had a remarkable effect on the adsorption capacity of the samples. ZIF-8 carbonized at 1000°C exhibited much higher adsorption capacity compared to the ZIF-8 carbonized at 600 and 1200°C.

The weak adsorption of ZIF-8 can be attributed to the small pore size (1.3 nm) which has the accessible pore sizes of 0.34 nm [53] as well as the positive surface charge (Fig. 5). After conversion to carbon the surface and bulk properties of ZIF-8 are modified; therefore, the resulting carbonized materials possess high negative surface charges, larger surface areas with broader pore size distributions. These features facilitate high adsorption of MB molecules

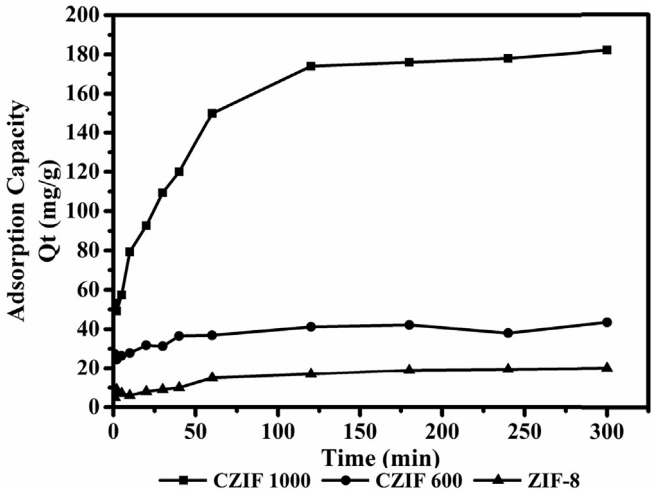

Fig. 7. Adsorption capacity of ZIF-8 and nano porous carbons for MB removal (initial dye concentration 100 ppm, adsorbent dosage 10 mg, solution volume 20 ml, initial pH = 5.5).

with nanoporous carbons. In addition, MB molecules can interact with the carbon surface because of the π-π interaction between MB molecules and sp^2 graphitic carbon in the carbon matrices. This is confirmed by Raman analysis shown in Fig. 6 [1]. The superior removal capacity of the nanoporous carbons compared to ZIF-8 is evidenced from Fig. 7, having adsorption capacity of 186.3 mg/g for CZIF1000, 43.5 mg/g for CZIF600 and 36.7 mg/g for CZIF 1200 compared with 19.5 mg/g adsorption capacity of ZIF-8.

The amount of MB uptake into the adsorbent materials was calculated using the following formula by simply considering the final and initial concentrations of dye solutions.

The percentage of dye removal (%) and the amount of dye adsorbed per unit of adsorbent (q) were calculated by the following equations:

$$\% = (C_i - C_e) \times \frac{100}{C_i} \quad (1)$$

Table 3
MB adsorption isotherm parameters n carbonized ZIF-8 prepared at 600 and 1000°C.

Sample	Q_e	Langmuir isotherm			Freundlich isotherm		
		K_L	Q_m	R^2	K_F	n	R^2
CZIF1000	186.3	0.86	185.2	0.999	126.6	10.52	0.7944
CZIF600	43.5	0.21	49.5	0.9975	35.6	17.1	0.7752

$$q = (C_i - C_e) \times \frac{V}{m} \quad (2)$$

where C_i and C_e are the initial and equilibrium concentrations (mg/l) respectively, V is the volume of dye solution (ml) and m is the weight of the adsorbents (g).

Table 2 summarises the comparison of adsorption capacities of MB on various MOF derived nanoporous carbons as well as activated carbons prepared from different sources. Nanoporous carbon derived from ZIF-67 exhibits the highest adsorption capacity in MB removal among the MOF derived carbon materials; whereas activated carbon from waste tea has the highest adsorption capacity for MB dye compared to activated carbons from other sources. The properties of activated carbon depends on the source material, therefore the adsorption capacities for dye removal differs for different kind of activated carbons. In most cases the activated carbons were treated and functionalized under harsh acidic conditions (or other chemical conditions) to make them suitable for adsorption. However, in this work, no further treatment was used and the ZIF-8 derived carbons were used directly after carbonization. For example, activated carbon derived from date palm leaflets was prepared using KOH activation followed by nitric acid oxidation to develop oxidized activated carbon. In addition, basic activated carbons were produced using ethylene diamine and propylene diamine to functionalize the surface of the carbons. The treated activated carbons had MB adsorption capacity in the range of 200–300 mg/g. The initial basic activated carbon had 270 mg/g adsorption capacity [54]. It is observed that ZIF-8 derived carbons show promising adsorption capacities in comparison with other materials. Therefore, untreated carbonized ZIF-8 with MB removal capacity of 186.3 mg/g is comparable with the other conventional carbon adsorbents for the removal of MB dye from water.

Table 2
Adsorption capacities of MB on various carbon based adsorbents.

Adsorbent	Adsorption isotherm	Adsorption pH	Carbonization T (°C)	Q_m (mg/g)	Reference
ZIF-67 derived carbon[a]	Langmuir	NA	600, 800°C	300.3, 500	[1]
Mixture of MIL-53 and MIL-58B carbon composite	Langmuir	NA	500, 600°C	74	[60]
MOF derived carbon (MIL-100 (Fe))	Langmuir	NA	500, 600°C	303.95	[37]
Polystyrene @ ZIF-8 core-shell microspheres	NA	NA	1000°C	NA	[61]
ZIF-8 derived carbon[a]	Langmuir	5.5	600°C	43.5	This study
ZIF-8 derived carbon[a]	Langmuir	5.5	1000°C	186.3	This study
ZIF-8 derived carbon[a]	NA	NA	800°C	59	[2]
Magnetic carbonized MOF-5[a]	Langmuir	6	900°C	292.4	[38]
AC[b] from date palm leaflets	Langmuir	7	550°C	270	[54]
AC from walnut shells	Redlich-Peterson	7	350–600°C	315	[62]
AC from cotton stalk	Langmuir	7	NA	193.5	[63]
AC from waste biomass	Langmuir	6	600°C	16.43	[64]
AC from waste tea	Langmuir	7	800°C	554.3	[65]
AC from Posidonia oceanica-dead leaves	Langmuir	6.5	600°C	285.7	[66]

[a] Prepared by direct carbonization.
[b] AC: Activated carbon.

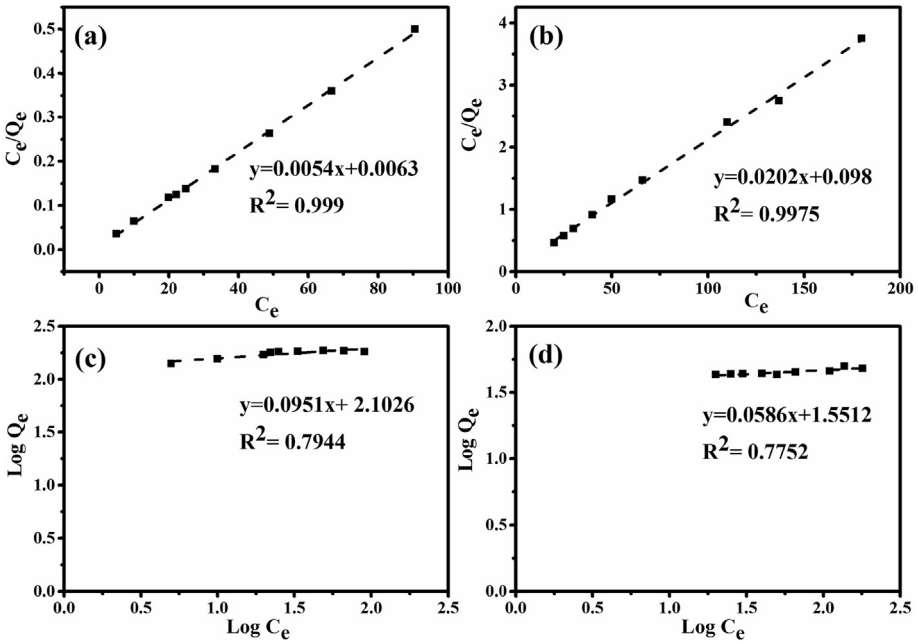

Fig. 8. Adsorption isotherms for adsorption of MB on carbonized ZIF-8 at 600 and 1000°C: (a) and (b) Langmuir isotherms, (c) and (d) Freundlich isotherms (adsorbent dosage 10 mg, solution volume 20 ml, initial pH = 5.5).

3.2.1. Adsorption isotherms

Analysis of the adsorption isotherm is of a great importance to describe how adsorbate molecules interact with the adsorbent surface. Equilibrium adsorption studies define the capacity of the adsorbent and also illustrate the adsorption isotherms by constants whose values express the surface properties and affinity of the adsorbents. The relationship between equilibrium data and either theoretical or practical equations is essential for interpretation and prediction of the extent of adsorption [55].

Among the adsorption isotherms the Langmuir and Freundlich models are the most common isotherms due to their simplicity and capability to describe experimental results in wide ranges of concentration (see the Supplementary Material) [56]. Adsorption isotherms were derived for CZIF 600 and CZIF 1000 to compare the results for different temperatures.

Table 3 shows the calculated values of Langmuir and Freundlich model's parameters. According to the graphs and calculations the equilibrium data showed a better fit to the Langmuir equation with r^2>0.99 addressing the homogeneous active sites and monolayer coverage of MB onto nanoporous carbons (Fig. 8a, b). The experimental data is verified by comparing the calculated maximum adsorption capacity (q_m) and equilibrium adsorption (q_e) (Table 3). The carbonized ZIF-8 at 1000°C shows an impressive adsorption capacity for MB dye with 186.3 mg/g which is almost 10 times and four times the amount adsorbed by carbonized ZIF at 600°C and ZIF-8 respectively.

The separation factor (R_L) was also calculated from Langmuir isotherms and is illustrated in Fig. 9. The favorable adsorption of Langmuir isotherm can be explained by means of a dimensionless separation factor R_L [57].

$$R_L = \frac{1}{1 + K_L C_i}$$

R_L values are described based on the following categories:

R_L	Type of isotherm
R_L>1	Unfavorable
R_L = 1	Linear
0<R_L<1	Favorable
R_L = 0	Irreversible

As illustrated in Fig. 9, since the RL values are all between zero and unity, thus it is confirmed the adsorption process over nanoporous carbons is favorable.

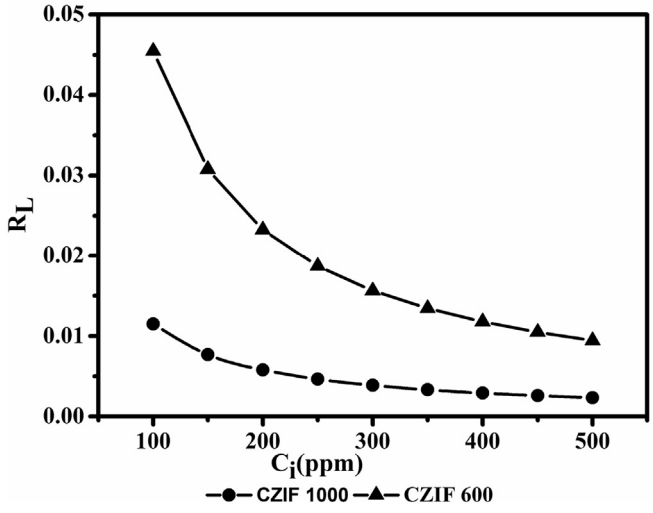

Fig. 9. RL values of the ZIF-8 derived nanoporous carbons at different initial concentrations (adsorbent dosage 10 mg, solution volume 20 ml, initial pH = 5.5).

Table 4
MB adsorption on carbonized ZIF-8 samples: kinetics parameters.

Sample	Pseudo first order			Pseudo second order			Intra particle diffusion		
	K_1 ($\times10^{-3}$) (min^{-1})	Q_e ($mg.g^{-1}$)	R^2	K_2 ($\times10^{-3}$) ($g.mg^{-1}.min^{-1}$)	Q_e ($mg.g^{-1}$)	R^2	K_i ($mg.g^{-1}.min^{-1}$)	C	R^2
CZIF1000	15.8	125.1	0.9503	0.38	188.67	0.9964	13.41	34.59	0.9808
CZIF600	15.2	16.87	0.9736	4.6	42.19	0.9935	1.66	23.63	0.9318

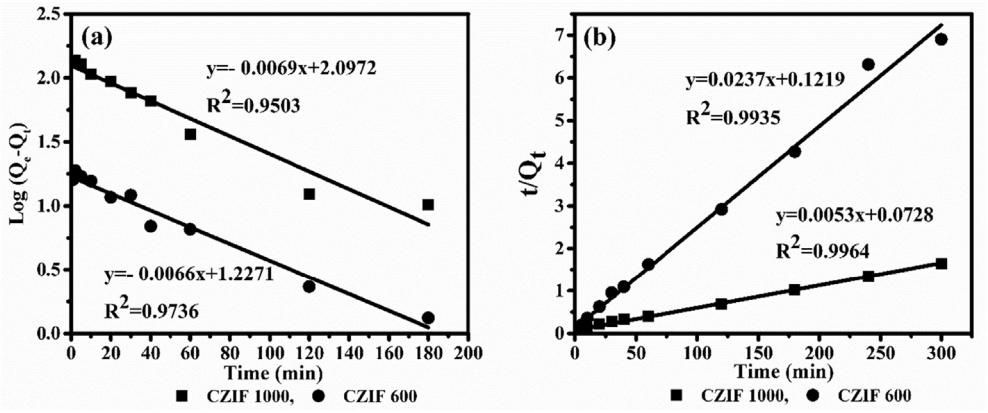

Fig. 10. Adsorption kinetics for adsorption of MB on CZIFs (initial dye concentration 100 ppm, adsorbent dosage 10 mg, solution volume 20 ml, initial pH = 5.5) (a) Pseudo first order and (b) Pseudo second order kinetics.

3.2.2. Adsorption kinetics

There are several adsorption kinetic models for defining the controlling mechanism of dye adsorption from aqueous solution. It is worth noting that the rate of adsorption of a particular molecule depends upon its mobility in the solution phase, the sorbent pore structure, the particle size, and the hydrodynamics of contact between the solution and the particle phase [58]. Pseudo-first order and Pseudo-second order models are widely used for the adsorption processes (see Supplementary Material). The adsorption kinetics calculation was performed for CZIF 600 and CZIF 1000 to compare the findings for two different temperatures.

The calculated kinetic parameters of the carbonized samples are given in Table 4. The experimental data was analysed by comparing the calculated q_t against time from the two kinetic models and thereafter was defined by linear regression. As it is shown in Fig. 10 the carbonized samples fitted kinetic models well. Nevertheless, the pseudo-second order model shows a better fit for the experimental data when comparing r^2 as it shows a higher r^2 (>0.99) compared to the pseudo-first order model. The calculated adsorption capacity from the latter is also very close to the experimental value. These results confirm the applicability of the pseudo-second-order equation. They also indicate that the sorption of MB into the nanoporous carbons follows the pseudo-second-order model.

3.2.3. Adsorption mechanism

Adsorption is usually controlled by either the liquid phase mass transport rate or the intraparticle mass transport rate. Weber and Morris [59] proposed the use of the intra-particle diffusion model to identify diffusion mechanisms of adsorption processes (see Supplementary Material).

The intraparticle diffusion plots of the nanoporous carbons provided a linear curve (Fig. S2). However, the plots did not pass through the origin which reflects that the intraparticle diffusion was constituted in the adsorption process but was not the only rate limiting step. Fitting the experimental data gives us three-phased graph. The line in the initial stage does not pass through the origin which indicates that the adsorption is mainly due to the external surface uptake instead of intra particle diffusion process. In this initial stage the adsorptive molecule diffuses through the solution to the external surface of the adsorbent or to the boundary layer diffusion where the adsorption rate is high. In the second stage, adsorption is faster reflecting the gradual adsorption step where intraparticle diffusion is rate-controlling. In the third section, diffusion remains relatively constant and the maximum adsorption is achieved [55].

The intraparticle rate constant (K_{id}) as can be seen from Table 3 is much higher for CZIF 1000 compared with CZIF 600 which can be attributed to a combination relationship between parameters such as specific surface areas and pore sizes of the adsorbents.

4. Conclusions

In this study, the effect of carbonization temperature on adsorption capacity of ZIF-8 for water treatment was investigated. Nano porous carbons were prepared by direct carbonization of ZIF-8 at 600°C, 1000°C and 1200°C. The SEM and TEM images proved that the nanoporous carbon particles retained the original morphology and structure after heat treatment. Zeta potentials provided information about the change in the surface charge of the samples addressing the negatively charged carbon nanoparticles compared with the positively charged ZIF-8 particles. The surface area of ZIF-8 decreased with increasing heat treatment temperature to 600°C and increased by raising the temperature to 1000°C; however, it decreased when the carbonization temperature was further increased to 1200°C. The pore size distribution became broader after carbonization which facilitated adsorption of MB. The adsorption studies revealed that nano porous carbon derived from ZIF-8 at 1000°C had outstanding adsorption capacity compared with ZIF-8. The isotherm and kinetics studies showed that the adsorption process followed the Langmuir model and agreed with pseudo-second order kinetic model. This study illustrates that the

heat treatment has significant effect on adsorption properties of ZIF-8 for the removal of organic pollutants from water.

Acknowledgement

This work was supported by the Australian Research Council through a Future Fellowship (Huanting Wang, Project no. FT100100192). The authors gratefully acknowledge the use of electron microscopes at Monash Centre for Electron Microscopy.

Appendix A. Supplementary data

Supplementary data related to this article can be found at http://dx.doi.org/10.1016/j.micromeso.2016.08.022.

References

[1] N.L. Torad, M. Hu, S. Ishihara, H. Sukegawa, A.A. Belik, M. Imura, K. Ariga, Y. Sakka, Y. Yamauchi, Direct synthesis of MOF-derived nanoporous carbon with magnetic Co nanoparticles toward efficient water treatment, Small 10 (2014) 2096–2107.
[2] B. Chen, G. Ma, D. Kong, Y. Zhu, Y. Xia, Atomically homogeneous dispersed ZnO/N-doped nanoporous carbon composites with enhanced CO2 uptake capacities and high efficient organic pollutants removal from water, Carbon 95 (2015) 113–124.
[3] B. Liu, H. Shioyama, H. Jiang, X. Zhang, Q. Xu, Metal–organic framework (MOF) as a template for syntheses of nanoporous carbons as electrode materials for supercapacitor, Carbon 48 (2010) 456–463.
[4] W. Chaikittisilp, M. Hu, H. Wang, H.-S. Huang, T. Fujita, K.C.W. Wu, L.-C. Chen, Y. Yamauchi, K. Ariga, Nanoporous carbons through direct carbonization of a zeolitic imidazolate framework for supercapacitor electrodes, Chem. Commun. 48 (2012) 7259–7261.
[5] R.R. Salunkhe, Y. Kamachi, N.L. Torad, S.M. Hwang, Z. Sun, S.X. Dou, J.H. Kim, Y. Yamauchi, Fabrication of symmetric supercapacitors based on MOF-derived nanoporous carbons, J. Mater. Chem. A 2 (2014) 19848–19854.
[6] M. Peer, A. Qajar, R. Rajagopalan, H.C. Foley, On the effects of confinement within a catalyst consisting of platinum embedded within nanoporous carbon for the hydrogenation of alkenes, Carbon 66 (2014) 459–466.
[7] A.N. Vasiliev, L.V. Golovko, V.A. Povazhny, E. Zlotnikov, J. Chen, J.G. Khinast, Functionalized nanoporous carbon as a catalyst for Suzuki coupling reactions, Microporous Mesoporous Mater. 101 (2007) 342–347.
[8] J.J. Lee, S. Han, H. Kim, J.H. Koh, T. Hyeon, S.H. Moon, Performance of CoMoS catalysts supported on nanoporous carbon in the hydrodesulfurization of dibenzothiophene and 4,6-dimethyldibenzothiophene, Catal. Today 86 (2003) 141–149.
[9] Z. Yang, Y. Xia, R. Mokaya, Enhanced hydrogen storage capacity of high surface area zeolite-like carbon materials, J. Am. Chem. Soc. 129 (2007) 1673–1679.
[10] X. Ma, L. Li, S. Wang, M. Lu, H. Li, W. Ma, T.C. Keener, Ammonia-treated porous carbon derived from ZIF-8 for enhanced CO2 adsorption, Appl. Surf. Sci. 369 (2016) 390–397.
[11] S. Gadipelli, Z.X. Guo, Tuning of ZIF-derived carbon with high activity, nitrogen functionality, and yield – a case for superior CO2 capture, ChemSusChem 8 (2015) 2123–2132.
[12] G.-P. Hao, W.-C. Li, D. Qian, A.-H. Lu, Rapid synthesis of nitrogen-doped porous carbon monolith for CO2 capture, Adv. Mater. 22 (2010) 853–857.
[13] S. Han, S. Kim, H. Lim, W. Choi, H. Park, J. Yoon, T. Hyeon, New nanoporous carbon materials with high adsorption capacity and rapid adsorption kinetics for removing humic acids, Microporous Mesoporous Mater. 58 (2003) 131–135.
[14] J.P. Ruparelia, S.P. Duttagupta, A.K. Chatterjee, S. Mukherji, Potential of carbon nanomaterials for removal of heavy metals from water, Desalination 232 (2008) 145–156.
[15] K. László, E. Tombácz, P. Kerepesi, Surface chemistry of nanoporous carbon and the effect of pH on adsorption from aqueous phenol and 2,3,4-trichlorophenol solutions, Colloids Surfaces A Physicochem. Eng. Aspects 230 (2003) 13–22.
[16] B. Xiao, K.M. Thomas, Competitive adsorption of aqueous metal ions on an oxidized nanoporous activated carbon, Langmuir 20 (2004) 4566–4578.
[17] A. Yazdankhah, S.E. Moradi, S. Amirmahmoodi, M. Abbasian, S.E. Shoja, Enhanced sorption of cadmium ion on highly ordered nanoporous carbon by using different surfactant modification, Microporous Mesoporous Mater. 133 (2010) 45–53.
[18] F. Güzel, H. Sayğılı, G.A. Sayğılı, F. Koyuncu, Elimination of anionic dye by using nanoporous carbon prepared from an industrial biowaste, J. Mol. Liq. 194 (2014) 130–140.
[19] B. Zheng, C. Lu, G. Gu, A. Makarovski, G. Finkelstein, J. Liu, Efficient CVD growth of single-walled carbon nanotubes on surfaces using carbon monoxide precursor, Nano Lett. 2 (2002) 895–898.
[20] Xu Yang, A. Tomita, T. Kyotani, The template synthesis of double coaxial carbon nanotubes with nitrogen-doped and boron-doped multiwalls, J. Am. Chem. Soc. 127 (2005) 8956–8957.
[21] M.P. Jensen, M.P. Mehn, L. Que, Intramolecular aromatic amination through iron-mediated nitrene transfer, Angew. Chem. 115 (2003) 4493–4496.
[22] A. Ahmadpour, D.D. Do, The preparation of active carbons from coal by chemical and physical activation, Carbon 34 (1996) 471–479.
[23] R. Ryoo, S.H. Joo, S. Jun, Synthesis of highly ordered carbon molecular sieves via template-mediated structural transformation, J. Phys. Chem. B 103 (1999) 7743–7746.
[24] T.-W. Kim, P.-W. Chung, I.I. Slowing, M. Tsunoda, E.S. Yeung, V.S.Y. Lin, Structurally ordered mesoporous carbon nanoparticles as transmembrane delivery vehicle in human Cancer cells, Nano Lett. 8 (2008) 3724–3727.
[25] J. Liu, T. Yang, D.-W. Wang, G.Q. Lu, D. Zhao, S.Z. Qiao, A facile soft-template synthesis of mesoporous polymeric and carbonaceous nanospheres, Nat. Commun. 4 (2013).
[26] Y. Wang, X. Wang, M. Antonietti, Y. Zhang, Facile one-pot synthesis of nanoporous carbon nitride solids by using soft templates, ChemSusChem 3 (2010) 435–439.
[27] N.L. Torad, M. Hu, Y. Kamachi, K. Takai, M. Imura, M. Naito, Y. Yamauchi, Facile synthesis of nanoporous carbons with controlled particle sizes by direct carbonization of monodispersed ZIF-8 crystals, Chem. Commun. 49 (2013) 2521–2523.
[28] N.A. Khan, Z. Hasan, S.H. Jhung, Adsorptive removal of hazardous materials using metal-organic frameworks (MOFs): a review, J. Hazard. Mater. 244–245 (2013) 444–456.
[29] S.H. Jhung, N.A. Khan, Z. Hasan, Analogous porous metal-organic frameworks: synthesis, stability and application in adsorption, CrystEngComm 14 (2012) 7099–7109.
[30] N.A. Khan, S.H. Jhung, Effect of central metal ions of analogous metal-organic frameworks on the adsorptive removal of benzothiophene from a model fuel, J. Hazard. Mater. 260 (2013) 1050–1056.
[31] N.A. Khan, B.K. Jung, Z. Hasan, S.H. Jhung, Adsorption and removal of phthalic acid and diethyl phthalate from water with zeolitic imidazolate and metal–organic frameworks, J. Hazard. Mater. 282 (2015) 194–200.
[32] H.-L. Jiang, B. Liu, Y.-Q. Lan, K. Kuratani, T. Akita, H. Shioyama, F. Zong, Q. Xu, From metal–organic framework to nanoporous carbon: toward a very high surface area and hydrogen uptake, J. Am. Chem. Soc. 133 (2011) 11854–11857.
[33] W. Chaikittisilp, K. Ariga, Y. Yamauchi, A new family of carbon materials: synthesis of MOF-derived nanoporous carbons and their promising applications, J. Mater. Chem. A 1 (2013) 14–19.
[34] S. Lin, Z. Song, G. Che, A. Ren, P. Li, C. Liu, J. Zhang, Adsorption behavior of metal–organic frameworks for methylene blue from aqueous solution, Microporous Mesoporous Mater. 193 (2014) 27–34.
[35] Y. Shao, L. Zhou, C. Bao, J. Ma, M. Liu, F. Wang, Magnetic responsive metal–organic frameworks nanosphere with core–shell structure for highly efficient removal of methylene blue, Chem. Eng. J. 283 (2016) 1127–1136.
[36] J.-Q. Jiang, C.-X. Yang, X.-P. Yan, Zeolitic imidazolate Framework-8 for fast adsorption and removal of benzotriazoles from aqueous solution, ACS Appl. Mater. Interfaces 5 (2013) 9837–9842.
[37] J.-D. Xiao, L.-G. Qiu, X. Jiang, Y.-J. Zhu, S. Ye, X. Jiang, Magnetic porous carbons with high adsorption capacity synthesized by a microwave-enhanced high temperature ionothermal method from a Fe-based metal-organic framework, Carbon 59 (2013) 372–382.
[38] C. Jiao, Y. Wang, M. Li, Q. Wu, C. Wang, Z. Wang, Synthesis of magnetic nanoporous carbon from metal-organic framework for the fast removal of organic dye from aqueous solution, J. Magnetism Magnetic Mater. 407 (2016) 24–30.
[39] N. Bakhtiari, S. Azizian, S.M. Alshehri, N.L. Torad, V. Malgras, Y. Yamauchi, Study on adsorption of copper ion from aqueous solution by MOF-derived nanoporous carbon, Microporous Mesoporous Mater. 217 (2015) 173–177.
[40] B. Liu, H. Shioyama, T. Akita, Q. Xu, Metal-organic framework as a template for porous carbon synthesis, J. Am. Chem. Soc. 130 (2008) 5390–5391.
[41] P. Zhang, F. Sun, Z. Xiang, Z. Shen, J. Yun, D. Cao, ZIF-derived in situ nitrogen-doped porous carbons as efficient metal-free electrocatalysts for oxygen reduction reaction, Energy & Environ. Sci. 7 (2014) 442–450.
[42] K. Kida, M. Okita, K. Fujita, S. Tanaka, Y. Miyake, Formation of high crystalline ZIF-8 in an aqueous solution, CrystEngComm 15 (2013) 1794–1801.
[43] Y. Shi, X. Zhang, L. Wang, G. Liu, MOF-derived porous carbon for adsorptive desulfurization, AIChE J. 60 (2014) 2747–2751.
[44] S. Sen Gupta, K.G. Bhattacharyya, Kinetics of adsorption of metal ions on inorganic materials: a review, Adv. Colloid Interface Sci. 162 (2011) 39–58.
[45] H.-x. Zhong, J. Wang, Y.-w. Zhang, W.-l. Xu, W. Xing, D. Xu, Y.-f. Zhang, X.-b. Zhang, ZIF-8 derived graphene-based nitrogen-doped porous carbon sheets as highly efficient and durable oxygen reduction electrocatalysts, Angew. Chem. Int. Ed. 53 (2014) 14235–14239.
[46] G. Srinivas, V. Krungleviciute, Z.-X. Guo, T. Yildirim, Exceptional CO2 capture in a hierarchically porous carbon with simultaneous high surface area and pore volume, Energy & Environ. Sci. 7 (2014) 335–342.
[47] N.S. Tabrizi, M. Yavari, Methylene blue removal by carbon nanotube-based aerogels, Chem. Eng. Res. Des. 94 (2015) 516–523.
[48] T. Zhang, L. Lin, X. Zhang, H. Liu, X. Yan, Z. Liu, K.L. Yeung, Facile preparation of ZIF-8@Pd-CSS sandwich-type microspheres via in situ growth of ZIF-8 shells over Pd-loaded colloidal carbon spheres with aggregation-resistant and leach-

proof properties for the Pd nanoparticles, Appl. Surf. Sci. 351 (2015) 1184–1190.
[49] S. Biniak, G. Szymański, J. Siedlewski, A. Świtkowski, The characterization of activated carbons with oxygen and nitrogen surface groups, Carbon 35 (1997) 1799–1810.
[50] Y. Liu, X. Xu, M. Wang, T. Lu, Z. Sun, L. Pan, Metal-organic framework-derived porous carbon polyhedra for highly efficient capacitive deionization, Chem. Commun. 51 (2015) 12020–12023.
[51] J.-H. Huang, K.-L. Huang, S.-Q. Liu, A.T. Wang, C. Yan, Adsorption of Rhodamine B and methyl orange on a hypercrosslinked polymeric adsorbent in aqueous solution, Colloids Surfaces A Physicochem. Eng. Aspects 330 (2008) 55–61.
[52] J. Goscianska, M. Marciniak, R. Pietrzak, Mesoporous carbons modified with lanthanum(III) chloride for methyl orange adsorption, Chem. Eng. J. 247 (2014) 258–264.
[53] G. Lu, S. Li, Z. Guo, O.K. Farha, B.G. Hauser, X. Qi, Y. Wang, X. Wang, S. Han, X. Liu, J.S. DuChene, H. Zhang, Q. Zhang, X. Chen, J. Ma, S.C.J. Loo, W.D. Wei, Y. Yang, J.T. Hupp, F. Huo, Imparting functionality to a metal–organic framework material by controlled nanoparticle encapsulation, Nat. Chem. 4 (2012) 310–316.
[54] E.I. El-Shafey, S.N.F. Ali, S. Al-Busafi, H.A.J. Al-Lawati, Preparation and characterization of surface functionalized activated carbons from date palm leaflets and application for methylene blue removal, J. Environ. Chem. Eng. 4 (2016) 2713–2724.
[55] E. Lorenc-Grabowska, G. Gryglewicz, Adsorption characteristics of Congo Red on coal-based mesoporous activated carbon, Dyes Pigments 74 (2007) 34–40.
[56] D. Sun, X. Zhang, Y. Wu, X. Liu, Adsorption of anionic dyes from aqueous solution on fly ash, J. Hazard. Mater. 181 (2010) 335–342.
[57] K.R. Hall, L.C. Eagleton, A. Acrivos, T. Vermeulen, Pore- and solid-diffusion kinetics in fixed-bed adsorption under constant-pattern conditions, Industrial Eng. Chem. Fundam. 5 (1966) 212–223.
[58] B. Okolo, C. Park, M.A. Keane, Interaction of phenol and chlorophenols with activated carbon and synthetic zeolites in aqueous media, J. Colloid Interface Sci. 226 (2000) 308–317.
[59] A.A. Jalil, S. Triwahyono, S.H. Adam, N.D. Rahim, M.A.A. Aziz, N.H.H. Hairom, N.A.M. Razali, M.A.Z. Abidin, M.K.A. Mohamadiah, Adsorption of methyl orange from aqueous solution onto calcined Lapindo volcanic mud, J. Hazard. Mater. 181 (2010) 755–762.
[60] A. Banerjee, R. Gokhale, S. Bhatnagar, J. Jog, M. Bhardwaj, B. Lefez, B. Hannoyer, S. Ogale, MOF derived porous carbon-Fe3O4 nanocomposite as a high performance, recyclable environmental superadsorbent, J. Mater. Chem. 22 (2012) 19694–19699.
[61] H.J. Lee, S. Choi, M. Oh, Well-dispersed hollow porous carbon spheres synthesized by direct pyrolysis of core-shell type metal-organic frameworks and their sorption properties, Chem. Commun. 50 (2014) 4492–4495.
[62] J. Yang, K. Qiu, Preparation of activated carbons from walnut shells via vacuum chemical activation and their application for methylene blue removal, Chem. Eng. J. 165 (2010) 209–217.
[63] H. Deng, L. Yang, G. Tao, J. Dai, Preparation and characterization of activated carbon from cotton stalk by microwave assisted chemical activation—Application in methylene blue adsorption from aqueous solution, J. Hazard. Mater. 166 (2009) 1514–1521.
[64] S. Karagöz, T. Tay, S. Ucar, M. Erdem, Activated carbons from waste biomass by sulfuric acid activation and their use on methylene blue adsorption, Bioresour. Technol. 99 (2008) 6214–6222.
[65] M. Auta, B.H. Hameed, Optimized waste tea activated carbon for adsorption of Methylene Blue and Acid Blue 29 dyes using response surface methodology, Chem. Eng. J. 175 (2011) 233–243.
[66] M.U. Dural, L. Cavas, S.K. Papageorgiou, F.K. Katsaros, Methylene blue adsorption on activated carbon prepared from Posidonia oceanica (L.) dead leaves: kinetics and equilibrium studies, Chem. Eng. J. 168 (2011) 77–85.